

Modern Physics Letters A
© World Scientific Publishing Company

The Trigger of the ATLAS Experiment

THOMAS SCHÖRNER-SADENIUS*

*CERN, Division EP
1211 Geneva 23, Switzerland
schorner@mail.desy.de*

Received (Day Month Year)

Revised (Day Month Year)

With the high bunch-crossing and interaction rates and potentially large event sizes the experiments at the LHC challenge data acquisition and trigger systems. Within the ATLAS experiment, a multi-level trigger system based on hardware and software is employed to cope with the task of event-rate reduction. This review article gives an overview of the trigger of the ATLAS experiment highlighting the design principles and the implementation of the system and provides references to more detailed information. In addition, first trigger-performance studies and an outlook on the ATLAS event-selection strategy are presented.

Keywords: LHC; ATLAS; trigger.

PACS Nos.: 07.05.Dz; 07.05.Hd; 07.05.Fb; 07.50.Qx.

1. Introduction

The Large Hadron Collider (LHC), which is currently being built at the European Organization for Nuclear Research (CERN) in Geneva¹, will collide proton beams at a center-of-mass energy of 14 TeV and a bunch-crossing rate of 40 MHz. At the design luminosity of $10^{34} \text{ cm}^{-2}\text{s}^{-1}$ about 25 proton-proton interactions will take place in every bunch-crossing. The amount of data that will arise from these conditions is enormous, making it impossible to store the information from all bunch-crossings or ‘events’ (note that the ATLAS experiment will have about 10^8 electronic channels). Therefore, the experiments at the LHC have to provide event selection or ‘trigger’ systems that select interesting or even ‘new’ physics processes and that help reject background processes and known (Standard Model) physics processes with large cross-sections.

Within the large LHC experimental collaborations (ATLAS, CMS, LHCb), the trigger is an important activity. The issues to be addressed range from hardware development, through software design and implementation, to the development of

*Now at Hamburg University, Institut für Experimentalphysik, Luruper Chaussee 149, 22761 Hamburg, Germany.

2 *Thomas Schörner-Sadenius*

event-selection criteria. In ATLAS, more than a hundred people are contributing to these efforts.

In this review article I will give an overview of the trigger system in the ATLAS experiment². After a short general introduction to the trigger in Section 2, I will turn in more detail to the various parts of the multi-level trigger, namely the level-1 trigger (Section 3) and the high-level triggers (Section 4). In Section 5 I will report on some trigger-performance studies. Finally, Section 6 is devoted to the ATLAS event-selection strategy as foreseen for LHC start-up in the year 2007.

2. The ATLAS Trigger

In the ATLAS experiment, the trigger is designed as a multi-level system which has to reduce the event rate from 40 MHz to about 200 Hz at which events (which will have an average size of the order of 1 MB) can be written to mass storage. Figure 1 gives an overview of the trigger system.

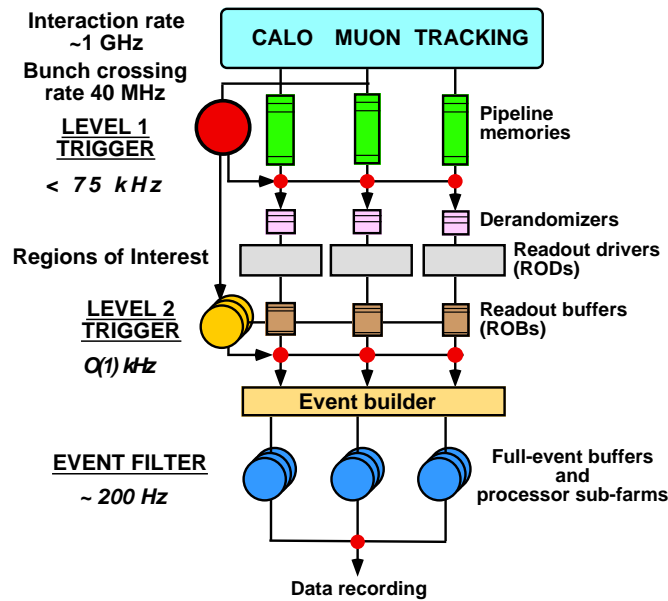


Fig. 1. A schematic view of the ATLAS trigger system.

The system is divided in three levels (from top to bottom in Fig. 1):

- The level-1 (LVL1) trigger is a hardware-based system which has to reduce the event rate of 40 MHz to below 75 kHz within a latency^a of 2.5 μ s. The

^aThe latency is the time needed to form and distribute the trigger decision. Its maximum value

LVL1 trigger makes its decision based on comparatively coarse information from only the ATLAS calorimeters and the muon trigger-chamber system.

- The level-2 (LVL2) trigger, which is part of the high-level trigger (HLT), is based on optimized software algorithms running in a processor farm and has to reduce the event rate to $\mathcal{O}(1)$ kHz. The LVL2 decision, which is based on the result of the LVL1 trigger, can take into account the information from all ATLAS subdetector systems which it retrieves as required. The LVL2 decision has to be ready after about 10 ms.
- The event filter (EF) is also part of the HLT and is implemented using software algorithms. In contrast to LVL2, the EF performs its task only after the complete event has been assembled in the event builder (EB). It uses comparatively complex algorithms, based on the offline software, and therefore can derive a very detailed event selection and classification, using the best available calibrations. The processing time of the EF for an event is of the order of a few seconds. EF-accepted events are written to mass-storage media.

3. The Level-1 Trigger

3.1. Principles

The task of the LVL1 trigger³ is to perform a first fast rate reduction, while selecting events with interesting signatures in the detector. Information from the ATLAS calorimeters and from dedicated fast muon trigger chambers, the resistive-plate chambers (RPC) and the thin-gap chambers (TGC), is used for this purpose. Consequently, the LVL1 trigger can be viewed in three parts, see Fig. 2: the calorimeter trigger, which receives the calorimeter information and prepares it for the event decision, the muon trigger which does the same for the information from the muon trigger chambers, and the LVL1 event-decision part implemented in the central trigger processor (CTP).

The information used to derive the LVL1 event decision is given in terms of the multiplicities of physics “objects” detected in the calorimeters or muon-trigger chambers which have sufficiently high transverse momentum (p_T). In the case of the calorimeter trigger, the objects in question are electrons/photons^b, τ leptons/hadrons, and jets. In addition, global energy sums (total transverse energy E_T , total missing transverse energy $E_{T,miss}$) can be considered.

The LVL1 trigger has to make and distribute its decision within a maximum latency of $2.5 \mu\text{s}$. During this time, the data fragments of all subdetectors are held in pipelined memories from where they are transferred to read-out buffers (ROBs)

is dictated by the bunch-crossing frequency and the length of the pipe-lines in which the event fragments are stored before LVL1 processing.

^bAt LVL1, electrons and photons cannot be distinguished, nor can hadrons and hadronic decays of τ leptons into narrow jets.

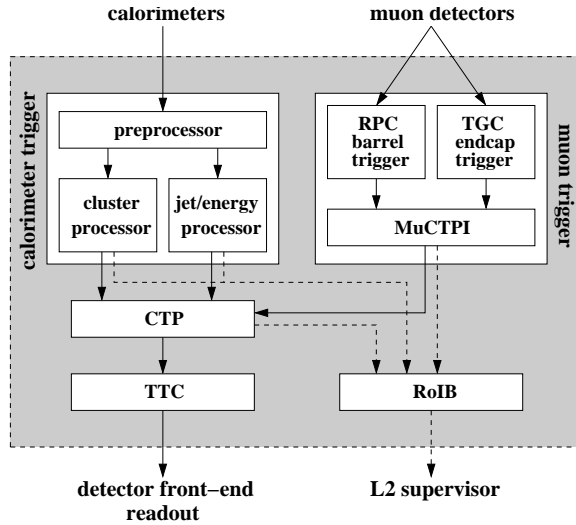
4 *Thomas Schörner-Sadenius*

Fig. 2. A schematic view of the LVL1 trigger. Solid lines between the different components indicate exchange of trigger-object multiplicity information, and dashed lines stand for Region-of-Interest. The Region-of-Interest builder (RoIB) is not part of the LVL1 trigger but is shown here for completeness. See text for more details.

upon LVL1 event acceptance (L1A). Currently about 1600 ROBs are foreseen in total for the ATLAS experiment. The L1A signal is also the starting point for the LVL2 trigger which is ‘seeded’ by LVL1 information transferred to it via the Region-of-Interest builder (RoIB). After the LVL2 decision the event fragments in the ROBs are either rejected, or they are passed to the event builder.

The TTC system, which is also indicated in Fig. 2, has the task of distributing timing and trigger signals to the read-out electronics. The signals it delivers comprise the LHC clock, synchronization signals, the L1A signal and test and calibration triggers. It will not be treated further in this article.

3.2. The calorimeter trigger

The ATLAS calorimeter system⁴ consists of the hadronic iron–scintillator tile sampling calorimeter in the barrel and the lead–liquid–argon sampling calorimeters in the barrel and the endcaps. In addition, the endcaps and the forward directions are equipped with hadronic endcap calorimeters with flat copper absorbers and copper/tungsten forward calorimeters, respectively. These latter two devices also use liquid argon as active medium.

The overall architecture of the calorimeter trigger³ can be seen in Fig. 3; it relies heavily on firmware-programmable FPGAs. On-detector electronics associated with each of the electromagnetic (EM) and hadronic (HA) calorimeters combines the signals from the individual cells by analogue summation. The results of this combination are analogue signals of 7200 approximately projective electromagnetic

and hadronic trigger towers (TT) with a granularity in $\eta \times \phi$ space of 0.1×0.1 . TTs are arranged so that a HA TT can be found projectively behind each EM TT.

The ~ 7200 TT signals are transmitted electrically to the preprocessor (PPr) electronics⁵ in the ATLAS electronics cavern where they are digitized in fast 10-bit ADCs. The preprocessor also performs bunch-crossing identification (BCID) using the pulse shapes of the TT signals, which for the LAr calorimeters have a length of several hundred ns. The importance of correct BCID lies in the fact that the long ($\mathcal{O}(100)$ ns) calorimeter signals have to be associated to a well-defined bunch-crossing in order to guarantee a sensible functioning of the trigger. After BCID, the PPr uses look-up tables to do a final calibration to 8-bit transverse energy (E_T) values, and presums EM and HA TTs in regions of $\Delta\eta \times \Delta\phi = 0.2 \times 0.2$ to so-called jet elements which will be used in the jet/energy trigger processor (see later).

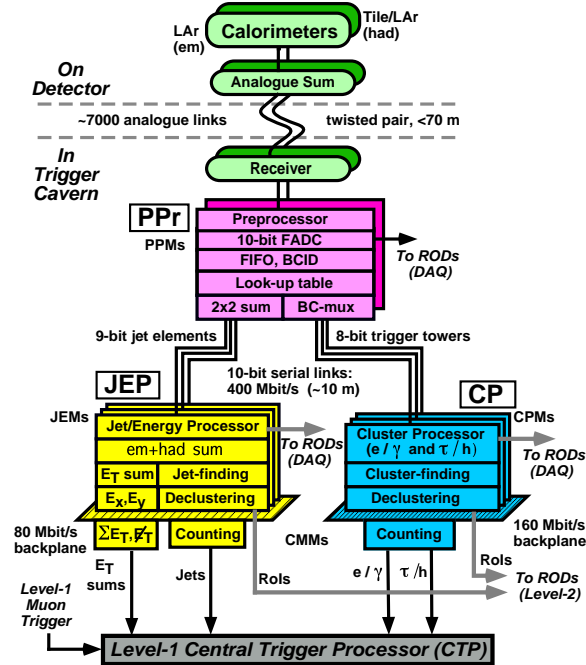


Fig. 3. A schematic view of the calorimeter trigger.

After the preprocessor, the signal path splits in two. The ~ 6400 TTs in the rapidity range $|\eta| < 2.5$ (corresponding to the inner-detector coverage and the region of highest EM-calorimeter granularity) are passed to the cluster processor (CP). The task of the CP is to identify electron/photon and τ /hadron candidates. The algorithm that identifies e/γ candidates has four elements⁶, see Fig. 4:

- (1) Clusters of 2×2 EM TTs which are local E_T maxima are searched for using

6 *Thomas Schörner-Sadenius*

a sliding-window technique. These 2×2 clusters are called Regions-of-Interest (RoIs) and serve as inputs to the higher trigger levels.

- (2) In a 2×2 cluster there are four pairs of two adjacent TTs. The pair with the highest sum E_T defines the transverse energy of the RoI.
- (3) The energy in the ring of 12 EM TTs surrounding the 2×2 RoI is used to define the EM isolation of the RoI.
- (4) Similarly, the 2×2 HA TTs behind the RoI and the 12 HA TTs behind the EM isolation ring are used to define the HA veto and isolation.

The E_T of each RoI is compared to one of 8 to 16 thresholds defined in the trigger configuration; each RoI passing one of the thresholds contributes to the multiplicity count for that threshold (if, in addition, the EM and HA isolation variables fulfill criteria associated with the threshold in question).

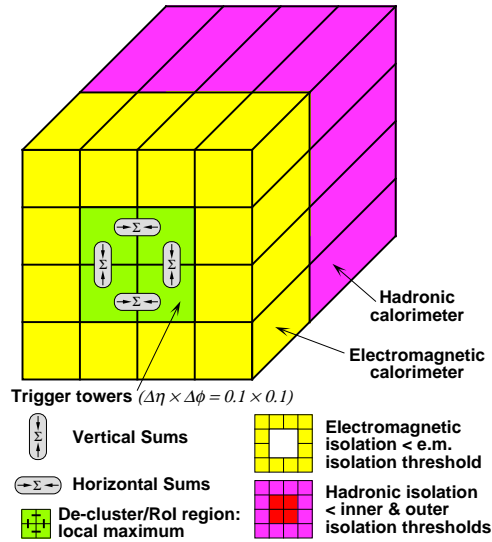


Fig. 4. The electron/photon algorithm. See text for details.

In the case of the τ /hadron algorithm, the RoI is again of size 2×2 , but now its E_T is derived from the highest- E_T 2×1 EM TT pair in the 2×2 cluster plus the energy of the 2×2 HA TT cluster behind it. In addition, criteria can be imposed on the electromagnetic and hadronic 12-TT isolation rings around the 2×2 core. The E_T of the τ /hadron RoIs is discriminated against 0–8 programmable thresholds (altogether, there exist 16 thresholds of which 8 to 16 may be taken by the e/γ trigger; only the remaining ones may be used by the τ /hadron trigger).

The results of the cluster processor are thus 8 to 16 multiplicities for e/γ candidates and 8 to 0 multiplicities for τ /hadron candidates. These multiplicities are sent to the central trigger processor (CTP) which makes the LVL1 event decision

for each bunch-crossing. In addition, for events selected by LVL1, all selected RoIs (defined by their locations in η - ϕ space and the transverse-energy threshold they passed) are transmitted to the higher trigger levels via the RoIB.

The second signal path from the preprocessor leads to the jet/energy processor (JEP). In this device, candidates for jets are searched for in the matrix of jet elements of 0.2×0.2 η - ϕ granularity (in the central rapidity range $|\eta| < 3.2$ – in the forward direction $3.2 < |\eta| < 4.9$ the algorithm works differently). This search leads to candidates for (normal) jets and forward jets. Like the cluster-processor objects, the jet candidates are located using a sliding-window technique, looking for an E_T maximum (RoI) in windows of 2×2 jet elements. Thresholds are applied for windows of 2×2 , 3×3 or 4×4 elements of $\eta \times \phi = 0.2 \times 0.2$ (window size independently programmable for each threshold). There are eight programmable jet- E_T and four forward-jet- E_T thresholds for which the total multiplicities are sent to the CTP. The jet RoIs are also sent to the RoIB for events selected by LVL1.

The jet/energy processor also evaluates the total scalar transverse energy and the missing transverse energy of each event, based on all 7200 TT signals over the acceptance of $|\eta| < 4.9$. These values, together with the total scalar E_T derived from the E_T of all jet RoIs, are also discriminated against programmable thresholds, the resulting information being passed to the CTP and, for selected events, to the RoIB.

3.3. The muon trigger

The task of the muon trigger³ is to find muon candidates which have transverse momenta in excess of one of six programmable thresholds (provided again via the LVL1 trigger menu).

The muon trigger consists of three separate devices⁷: The RPC trigger prepares the information collected in the resistive-plate chamber (RPC) detectors in the ATLAS barrel ($|\eta| < 1.05$), the TGC trigger does the same for the thin-gap chamber (TGC) information in the forward region ($1.05 < |\eta| < 2.4$), and the muon-to-CTP interface (MuCTPI) collects information from both RPC and TGC triggers, refines it and sends the results to the CTP and to the RoIB.

As can be seen from Fig. 5, there exist three so-called (RPC or TGC) ‘stations’, each of which contains two planes of chambers (the innermost TGC station has three planes). In the absence of inefficiencies and acceptance gaps, this results in six η and ϕ coordinates for each ‘view’.

The algorithm that searches for muon candidates (in the barrel) works as follows⁸: Each hit found in the middle RPC station (RPC2) is extrapolated to the innermost RPC station (RPC1) along a straight line through the nominal interaction point, and a ‘coincidence window’ is defined around the point where this line hits the RPC1 station. Since the ATLAS magnetic field will deflect charged particles, the size of the coincidence window defines the transverse momentum, p_T , of muon tracks that can be triggered upon. A low- p_T muon candidate is found if there is at least one hit in the coincidence window and if in at least one of the

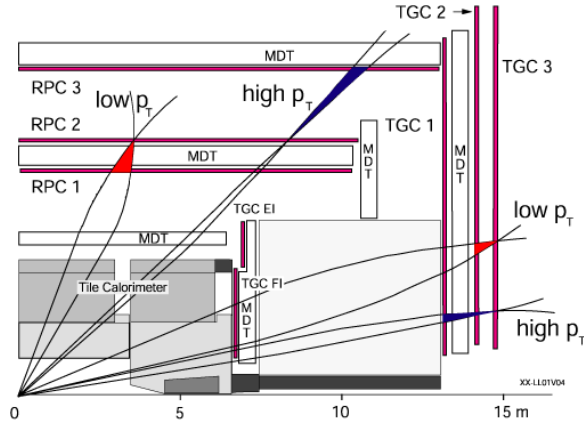


Fig. 5. The LVL1 muon trigger: An rz view of a quarter of the ATLAS detector. Some muon candidate tracks are shown to highlight the muon trigger algorithm which is explained in the text. ‘MDT’ stands for the ‘Monitored Drift Tubes’ precision detectors which form the muon spectrometer in the barrel.

stations RPC1 and RPC2 hits can be found in both planes and in both views. In addition, if there is a coinciding hit in at least one of the planes of the outermost station RPC3, a high- p_T muon candidate has been found. These low- and high- p_T candidates are the muon trigger Regions-of-Interest.

Six programmable sets of coincidence windows are defined, each corresponding to a different p_T threshold; three of the thresholds are reserved for low- p_T coincidence windows (5 to ~ 10 GeV), and three for high- p_T coincidences (~ 10 to 35 GeV). Threshold values are designed such that they correspond to an efficiency of 90%.

The muon trigger is arranged in 208 sectors, each of which can deliver a maximum of two muon-candidate RoIs to the MuCTPI. In case of more than two candidates in one sector, the two with the highest p_T values are used and a flag is set. The MuCTPI⁹ calculates the multiplicity for each p_T threshold, applying an algorithm to avoid double-counting of muons, and passes the resulting multiplicity values to the CTP for LVL1 event decision. In addition, for selected events, up to 16 muon RoIs, defined by their position in $\eta \times \phi$ space and the transverse-momentum threshold they passed, are sent to the high-level triggers via the RoIB.

3.4. LVL1 event decision and LVL1/LVL2 interface

The LVL1 event decision³ is based on the multiplicities of high- p_T objects sent to the CTP from the calorimeter trigger and the MuCTPI together with threshold information on global energy sums. The decision is derived in two steps. In a first step, the delivered multiplicities are discriminated against multiplicity requirements or ‘conditions’, leading to truth values ‘yes’ or ‘no’ for each condition defined in the LVL1 trigger menu. Then, the condition truth values are logically combined to

complex ‘trigger items’ which represent signatures to be triggered by LVL1. Two examples for such items are

‘at least two e/γ candidates with $p_T > 10$ GeV’
‘at least one jet with $p_T > 100$ GeV and $E_{T,miss} > 400$ GeV’.

In the first case, the trigger item consists of only one trigger condition; in the second example, the item consists of the logical ‘AND’ of two trigger conditions. The LVL1 event decision is derived from the logical values of all trigger items by applying a logical ‘OR’ (see Section 6 for an overview of possible signatures).

The final implementation of the CTP is currently being designed. There exists however a demonstrator prototype, the CTP-D, which has been used for feasibility studies and tests¹⁰. The CTP-D receives 32 input signal bits encoding the multiplicities of calorimeter/muon trigger objects. The multiplicity discrimination is implemented using look-up tables, and the logical combination of conditions to items takes place in programmable devices. Up to 32 items can be built. The result of the CTP-D includes also prescaling and a simple dead-time algorithm for all 32 items.

In contrast to the CTP-D, the core functionality of the final CTP can probably be implemented in one single programmable device, thanks to the speed and capacity progress for electronic devices over the past few years. 160 input bits are foreseen, allowing for a much higher number of multiplicities to be encoded and thus for a greatly increased trigger flexibility, compared to the 32 input bits of the CTP-D. Also the number of trigger items will be increased from 32 (CTP-D) to 160 or more.

The LVL2 processing, which will be explained in detail below, starts from the RoIs selected by the LVL1 trigger. As mentioned above, these RoIs are sent to the Region-of-Interest builder¹¹ (RoIB) over eight fast links (one for the muon trigger, six for the calorimeter trigger, and one for the CTP information). The RoIB takes all eight data fragments and concatenates them into one single data fragment which is transferred to the LVL2 trigger supervisor assigned for the event. This operation must be performed at a full LVL1 output rate of up to 75 kHz without introducing significant dead-time into the system.

4. The High-Level Trigger

4.1. Overview

The ATLAS high-level trigger¹² (HLT) consists of the level-2 (LVL2) trigger and the event filter (EF) which are both implemented as pure software triggers running in processor farms. Figure 6 gives an overview of the data flow in the HLT environment.

The LVL2 supervisor (L2SV) computers, about ten of which are envisaged for the final system, receive the LVL1 result from the RoIB and assign events to processors in the LVL2 farms. Note that no processing node (not even L2SV nodes) sees the full LVL1 output rate. In the LVL2 farm processors, the LVL2 processing unit (L2PU)

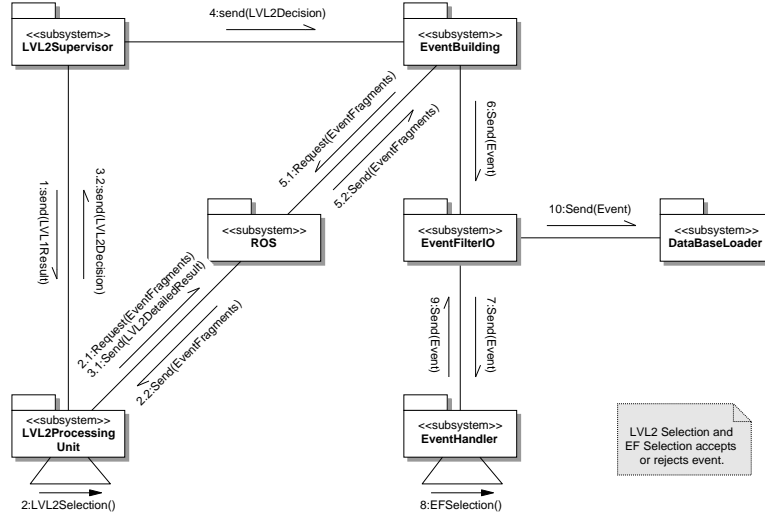
10 *Thomas Schörner-Sadenius*

Fig. 6. Outline of the HLT data flow. See text for more details.

is running which forms the interface between the L2SV, the read-out subsystem (ROS^c) and the true HLT selection software (see Section 4.3). During the selection procedure, information from various subdetectors can be retrieved from the ROS. In order to minimize the idle-time while waiting for the response to data requests to the ROS, LVL2 will allow for multi-threading of selection tasks in the LVL2 processors. The decision of the LVL2 selection is sent back to the corresponding L2SV which, in the case of a positive LVL2 decision, passes it to the event building. LVL2 has a processing time of about 10 ms and has to reduce the incoming LVL1 rate to $\mathcal{O}(1)$ kHz.

Event building is the data-acquisition step in which all event fragments from all ATLAS subdetectors are requested from the ROS and assembled to give a full ATLAS event. The event is then sent to the EF. Here, the EventFilterIO distributes newly arriving events to one of the EF processors. In these processors, the EventHandler supports the actual EF selection (and classification) after which, in case of a positive EF result, the event will be written to the ATLAS mass-storage devices. The processing time of the EF is limited to a few seconds; the EF output rate goal is of the order of 200 Hz.

4.2. HLT Selection Principles

The LVL2 and the EF share two important principles:

- In both levels, the selection procedure starts with a limited number of LVL1

^cThe ROS aggregates several (typically 3) ROBs (see Section 3.1) in a single unit.

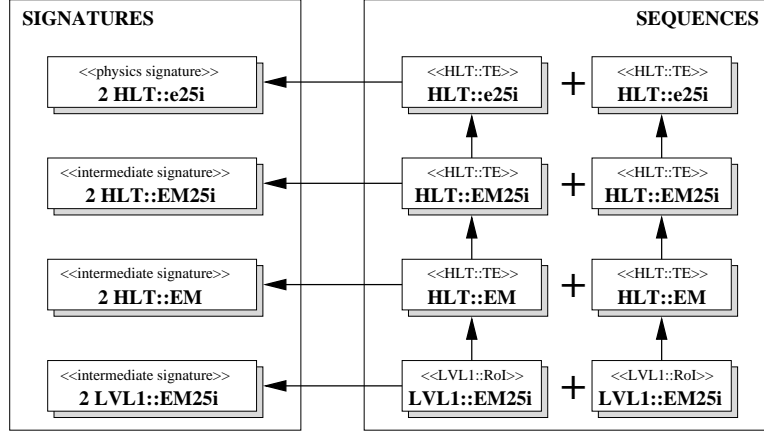


Fig. 7. Overview on the step-wise selection procedure for an example physics signature. See text for more details.

(or LVL2, in case of the EF) RoIs which “seed” the next level.

- In both levels, the event decision is derived in a step-wise procedure in which the initial hypothesis is either confirmed or rejected. In each step, the existing information is refined by accessing data from more subdetectors or by performing algorithmic work on the present information. At the end of each step it is checked whether the present data still allow for the event to be triggered. If not, the event is rejected.

The advantage of these two principles is that they allow for fast and light-weight HLT decisions: Working the data-driven way – i.e. starting with only a few RoIs – significantly reduces the amount of data to be moved (at LVL2) and processed (at LVL2 and in the EF) compared to a scheme where first all data are collected and then a global decision based on processing the full event data is performed. Only the data necessary for the next step are gathered and/or processed. Since an event can be rejected after each of the (small) steps, the amount of time invested in rejected events on average is comparatively small.

Figure 7 highlights the step-wise selection procedure for the ‘2e25i’ example physics signature (i.e. for a trigger requirement of two or more isolated electrons with an E_T of at least 25 GeV): In a first step, all existing LVL1 RoIs are collected, and it is tested whether they are able to fulfill the event signature ‘2 LVL1::EM25i’ which requires two isolated LVL1 electromagnetic-calorimeter clusters of at least 25 GeV. If this is the case, algorithms are used to refine the information contained in the ‘LVL1::EM25i’ RoIs by applying, for example, a shower-shape analysis to the clusters. This analysis might be able to distinguish between EM showers due to single electrons or photons, and EM clusters resulting from $\pi^0 \rightarrow \gamma\gamma$ decays within jets. Trigger elements passing this analysis step may thus be regarded as real HLT

electromagnetic clusters and are denoted as ‘HLT::EM’. If two such trigger elements can be found, the next intermediate signature ‘2 HLT::EM’ can be satisfied and the selection process will be continued.

In a further step, algorithms might test whether the clusters have sufficient transverse energy (> 25 GeV) and are sufficiently well isolated (suffix ‘i’), possibly leading to the creation of trigger elements ‘HLT::EM25i’ for one or both of the ‘HLT::EM’ trigger elements. In case two TEs ‘HLT::EM25i’ are present, the next intermediate signature ‘2 HLT::EM25i’ can be satisfied, and the selection process will be continued. Finally it might be checked whether there are tracks pointing to the calorimeter clusters, indicating electrons (that thus can be distinguished from photons) and leading to the creation of trigger elements ‘HLT::e25i’. If tracks can be found for both ‘HLT::EM25i’ TEs, the physics signature ‘2 HLT::e25i’ can be satisfied and the event will be triggered.

4.3. HLT Selection Software

The central part of the HLT clearly are the decision steps performed by the selection software running in the L2PU and in the EventHandler. This is the HLT selection software (HLTSSW). An overview of the core selection software, together with its connections and interfaces to other software pieces, is shown in Fig. 8.

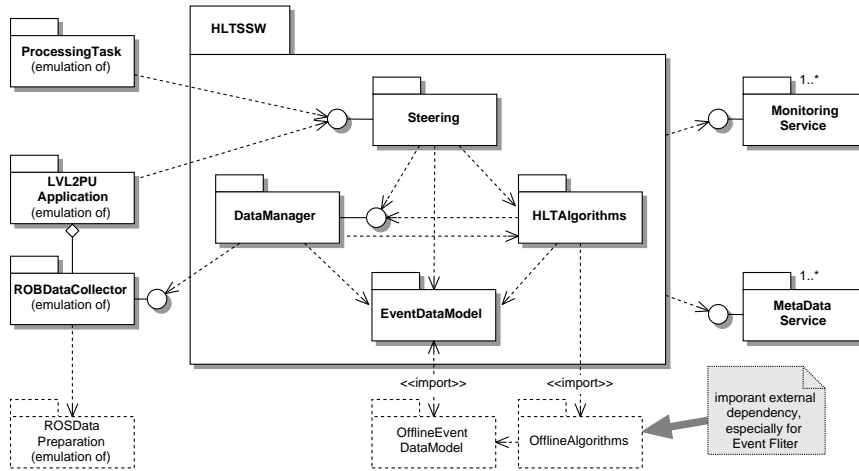


Fig. 8. Overview of the HLT selection software.

The HLTSSW consists of four parts or ‘packages’¹³:

- The Steering¹⁴ controls the selection software. It organizes the correct order of the HLT algorithms processing such that the required data are produced and the trigger decision is obtained.

- The event data are structured according to the EventDataModel (EDM). The EDM¹⁵ covers all data entities in the event and their mutual relations (raw data, LVL1 result and RoIs, LVL2 and EF results).
- The HLT Algorithms¹⁶ are used by the Steering to process the event information and to obtain the data on the basis of which the event decision is taken. LVL2 algorithms are special developments, designed for running in the time-critical LVL2 environment, whereas for the EF selection mostly algorithms adapted for the offline reconstruction will be used.
- The DataManager is responsible for handling all event data during the trigger-selection procedure and, in particular, for retrieving the necessary additional data from the ROS.

The HLT selection software has been developed in the ATLAS offline computing framework Athena¹⁷, which in turn is based on the Gaudi framework¹⁸. This seems natural for the EF which is running offline-reconstruction algorithms, but required some adaptations of the LVL2 online-software environment. This disadvantage, however, has to be compared to the advantages: First, a common HLT framework allows for a flexible boundary between LVL2 and EF, facilitating latency and rejection trade-offs between these two systems. Second, the offline framework is the standard user and analysis framework in ATLAS. Thus anybody capable of using this framework should be able to develop selection and reconstruction algorithms not only for EF, but also for LVL2.

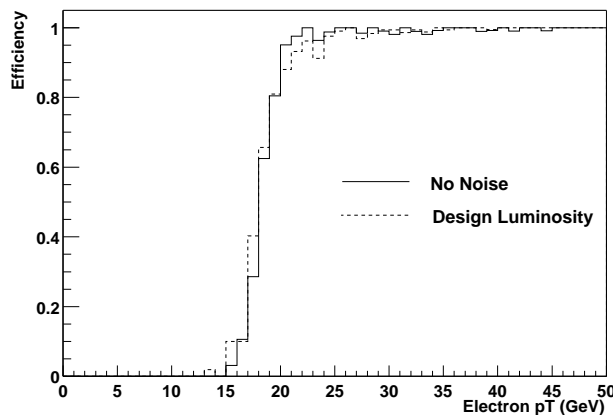


Fig. 9. LVL1 efficiency for single electrons as a function of their transverse energy, using a 17 GeV threshold for different scenarios. See text for more details.

5. Trigger-Performance Studies

Already some time ago thorough trigger-performance studies were carried out in ATLAS; they are documented, for example, in the HLT Technical Proposal¹⁹. In ad-

dition, the recently published HLT Technical Design Report¹² has initiated a large number of studies which involve improved knowledge compared to the Technical Proposal and which therefore promise improved insight into the ATLAS physics potential. These studies range from validations of the LVL1 trigger simulation (which provide the input to the HLT studies), through feasibility studies for the HLT architecture, to stability and rate tests for the selection software. All results shown below are taken from the Technical Design Report, if not stated differently.

Figure 9 shows, as a function of the electron E_T , the simulated trigger efficiency for electrons using a trigger for single EM-calorimeter objects²⁰. An E_T cut of 17 GeV has been applied on the raw measured energy in order to achieve an efficiency of 95 % for the nominal threshold of 20 GeV. A sharp rise of the efficiency around the nominal threshold value can be observed. The behavior is similar for two scenarios considered, namely the pure signal without calorimeter noise or pile-up added (label ‘no noise’) and high (LHC design) luminosity ($10^{34}\text{cm}^{-2}\text{s}^{-1}$, labeled ‘Design Luminosity’).

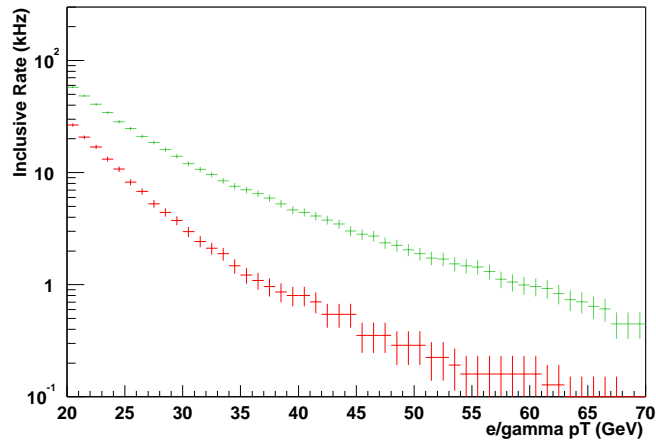


Fig. 10. LVL1 rate for the inclusive EM-cluster trigger versus E_T threshold without (top) and with (bottom) isolation requirements at low luminosity $2 \cdot 10^{33}\text{cm}^{-2}\text{s}^{-1}$. See text for more details.

Figure 10 shows, as a function of the E_T threshold, the expected trigger rates for a LVL1 calorimeter trigger for single electrons for $2 \cdot 10^{33}\text{cm}^{-2}\text{s}^{-1}$. The E_T threshold scale is defined such that the efficiency for genuine electrons with E_T equal to the cited value is 95 %. The top line indicates the rate for the case of no isolation required; the bottom line shows the expected rate with isolation cuts applied on the electromagnetic calorimeter cluster. The difference between the two lines demonstrates the ability of the isolation criteria to reduce the dominating rate contribution from misidentified jets.

Similar studies are currently being performed for the LVL1 muon trigger.

Table 1 shows an example of a HLT study taken mainly from the Technical

Proposal¹⁹ in which the expected performance of the isolated-electron HLT trigger was tested²¹. Shown are, separately for low and design luminosity, the expected trigger rates and efficiencies and first timing measurements^d. In this table, the rates, efficiencies ϵ and timings are shown for the various steps of the HLT electron-trigger process: ‘LVL2 Calo’ corresponds to the precision reconstruction of the EM calorimeter cluster, and to the measurement of the transverse energy of the cluster. ‘LVL2 Precision’ and ‘LVL2 TRT’ refer to two different track-finding algorithms involving the precision silicon and pixel detectors and the ATLAS transition-radiation tracker (TRT), respectively. ‘LVL2 Matching’ denotes the effort to match the track and cluster information in position and energy. ‘EF Calo (Matching)’ are the EF equivalents to ‘LVL2 Calo (Matching)’, and ‘EF ID’ stands for RoI-seeded track search in the ATLAS inner (tracking) detector (ID). Also shown in the table (column $2 \cdot 10^{33}$) are first rate studies from the HLT Technical Design Report for some of the steps mentioned above^{20,22}; the efficiencies are expected to be between the values for $10^{33} \text{cm}^{-2} \text{s}^{-1}$ and $10^{34} \text{cm}^{-2} \text{s}^{-1}$.

Table 1. Overview of HLT trigger rates, efficiencies and timings for the single electrons at different luminosities. See text for more explanation.

Lumi [$\text{cm}^{-2} \text{s}^{-1}$]	10^{34}			10^{33}			$2 \cdot 10^{33}$
Trigger Step	Rate [Hz]	ϵ [%]	Timing	Rate [Hz]	ϵ [%]	Timing	Rate [Hz]
LVL1 output	21700	94.6	–	11000	92.6	–	12000
LVL2 Calo	3490	97	0.3 ms	1100	96	0.2 ms	2114
LVL2 Precision	620	90	13 ms	150	92	6 ms	–
LVL2 TRT	1360	90	1.2 s	360	89	210 ms	–
LVL2 Matching	460	85	–	140	88	–	137
EF Calo	313	84	0.63 s	85	86	0.56 s	–
EF ID	149	79	71 s	57	82	1.6 s	–
EF Matching	117	78	–	41	81	–	30

The efficiencies are shown for electrons of 20/25/30 GeV transverse energy for $10^{33}/2 \cdot 10^{33}/10^{34} \text{cm}^{-2} \text{s}^{-1}$, respectively, over the calorimeter rapidity range of $|\eta| < 2.5$. The timing measurements, which were performed on various computing platforms with the results being transformed to a 500 MHz Pentium PC equivalent (year 2000), give the latency within which 95 % of all events were processed; median numbers are in some cases much shorter. The numbers were derived for the purely algorithmic part of the trigger process, excluding as much as possible input/output processes and data preparation. Efficiency and rate values for the HLT are given with respect to the LVL1 efficiency of about 95 % and the LVL1 output rates which are also given in the table. The final rates for the two lower-luminosity scenarios

^dNote that at the time of the Technical Proposal, the low luminosity scenario – in contrast to today’s assumption of $2 \cdot 10^{33} \text{cm}^{-2} \text{s}^{-1}$ – was assuming $10^{33} \text{cm}^{-2} \text{s}^{-1}$.

are in acceptable agreement with the foreseen trigger menu, see Section 6.

Table 2 shows the estimated output rates of the LVL2 muon trigger algorithm μ FAST^{12,23} for various physics processes, applying a p_T threshold of 6 or 20 GeV^e for the $10^{33}\text{cm}^{-2}\text{s}^{-1}$ or $10^{34}\text{cm}^{-2}\text{s}^{-1}$ luminosity scenario, respectively. For this study the rapidity of the muons was limited to the barrel region $|\eta| < 1$. The μ FAST algorithm was especially developed for the LVL2-online environment and relies on information from both the muon trigger chambers (RPCs) and the muon precision chambers (MDTs). It is seeded by LVL1 RPC RoIs which help to define a ‘road’ around the μ trajectory. The MDT tubes that are hit by such a road are selected, and a straight-line fit is placed through all selected tubes from which an estimate of the μ p_T can be derived.

Table 2. Rates for the LVL2 muon trigger algorithm μ FAST with a threshold of 6 (20) GeV for low(high) luminosity for various physics processes.

Physics Process	$10^{33}\text{cm}^{-2}\text{s}^{-1}$ [kHz]	$10^{34}\text{cm}^{-2}\text{s}^{-1}$ [kHz]
π /K decays	3.00	0.07
b decays	0.90	0.09
c decays	0.50	0.04
$W \rightarrow \mu\nu$	negligible	0.02
cavern background	negligible	negligible
Total	4.40	0.22

Figure 11 shows, as a further result from the new HLT studies, the LVL2 efficiency for prompt muons and for K/ π decays in flight. The left plot shows the efficiency for the μ FAST algorithm; the efficiency curves were derived with a more complete ‘combined’ muon algorithm which combines information from the ATLAS tracking detectors and the muon spectrometer. It is clearly visible that the combined algorithm provides increased separation power between prompt muons and muons from K/ π decays which in turn leads to a decreased rate for muons with $p_T > 6$ GeV of 2.1 kHz at $10^{33}\text{cm}^{-2}\text{s}^{-1}$.

Further studies, for example those investigating technical details of the HLT architecture, cannot be discussed here. Please refer to some recent publications on these issues²⁴.

6. ATLAS Event-Selection Strategy

The aim of the ATLAS event selection is to be as open and efficient as possible for new physics processes, while preserving good rejection power against well-known background and Standard Model processes with large cross-sections²⁵. This aim

^eNote that according to the present trigger configuration ideas presented in Section 6 no inclusive 6 GeV–muon trigger is foreseen anymore for the low luminosity scenario.

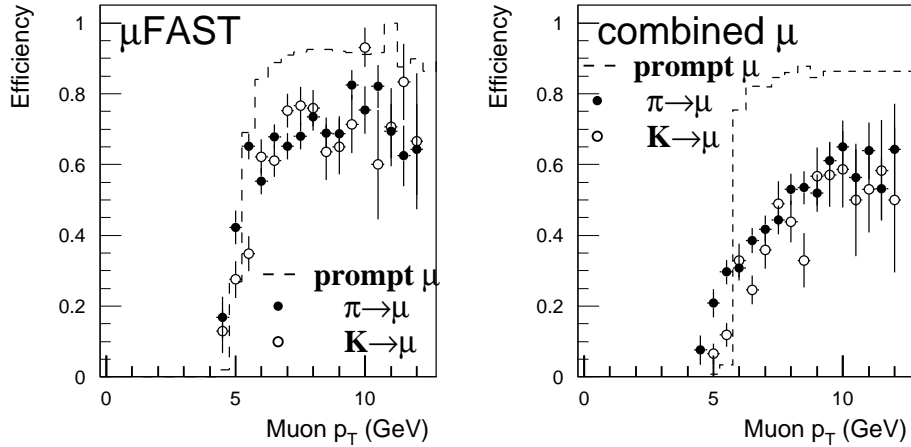


Fig. 11. The efficiency at LVL2 with respect to LVL1 of the μ FAST and the combined muon algorithm for prompt muons and muons from K/π decays in flight. See text for more details.

shall be achieved by designing a selection based on low multiplicities of high- p_T objects. It is foreseen to implement the following triggers^f:

- Inclusive and di-lepton triggers will cover large parts of the Standard Model and the discovery physics programme of ATLAS. Examples of processes accessible with them are associated Higgs production $t\bar{t}H$, $H \rightarrow ZZ(WW)$ decays, top physics, or $Z \rightarrow l\bar{l}$ decays (also needed for detector calibration purposes). The B-physics programme relies to a large extent on muon triggers augmented by more exclusive selections.
- There will be a variety of jet triggers, with required multiplicities between one and four jets. The thresholds will be highest for the inclusive jet trigger, of the order of 400 GeV (on HLT); for the four-jet trigger, thresholds of around 100 GeV are envisaged. In addition, jets in the very forward direction, close to the proton beams, can be used to trigger. The purpose of the jet triggers is mainly QCD studies (and background determination of search channels), but also new physics signatures can be selected with them (for example new resonances with the di-jet trigger or R-parity violating supersymmetry).
- Triggers based on the missing transverse energy and the total transverse energy are vital parts of the search for new physics, for example for invisibly-decaying particles and supersymmetric signatures. The threshold for the missing- E_T trigger is assumed to be about 150 GeV, and the total- E_T trigger should fire at energies above 1 TeV approximately.

^fHere only the unrescaled part of the trigger menu is mentioned. There are numerous other (prescaled) triggers which will be used for more exclusive selections, for example in the area of B physics, or for monitoring, calibration and efficiency-determination purposes.

- In addition to the above, there are a number of ‘mixed’ triggers foreseen, in which leptons and jets are combined with missing transverse energy, for example.

The threshold values of the various triggers mentioned above are mostly the result of physics studies involving leading-order Monte Carlo predictions and (incomplete) simulations of the ATLAS detector and its trigger. They represent compromises between selection efficiency and rate reduction needs and might well be subject to future changes, due to more precise theoretical predictions, better ATLAS detector simulations and a better knowledge of the ATLAS detector layout.

All in all, it is foreseen that ATLAS will trigger on a set of about 100 physics signatures, including prescaled triggers and calibration and monitoring triggers. The total rates for the LVL1 trigger and the HLT that are currently aimed for are 25 kHz and 200 Hz, respectively, taking into consideration various uncertainties on the predicted rates and the reduced rate ability ATLAS has to cope with during the start-up phase due to financial problems. Table 3 gives estimates of rates for the most important unprescaled trigger signatures²⁶ for the low luminosity scenario ($2 \cdot 10^{33} \text{cm}^{-2} \text{s}^{-1}$). The numbers quoted in this table are mainly derived from older predictions (for example from the Technical Proposal¹⁹) for the original low-luminosity scenario $10^{33} \text{cm}^{-2} \text{s}^{-1}$ which were scaled appropriately.

Table 3. Rate estimates for various trigger signatures at LVL1 and HLT for the low-luminosity scenario $2 \cdot 10^{33} \text{cm}^{-2} \text{s}^{-1}$. ‘EM’, ‘MU’ and ‘J’ stand for LVL1 electron/photon, muon or jet candidates, respectively. ‘xE’ denotes missing transverse energy at both LVL1 and HLT. ‘e’, ‘ γ ’, ‘ μ ’ and ‘j’ denote electron, photon, muon and jet candidates at HLT. Only an extract from the complete inclusive unprescaled trigger menu is shown here; τ /hadron triggers, forward-jet triggers and pure energy triggers are completely omitted. The ‘2MU6’ threshold is under discussion; a threshold value as low as possibly allowed by the muon-trigger design will be used. The ‘mass’ that is referred to in the ‘2MU6’ line is the invariant mass of the di-muon system which may be required to be close to the mass of the $J \setminus \Psi$, for example, from the decay of which the muons are supposed to come.

LVL1 Signature	LVL1 Rate [kHz]	HLT Signature	HLT Rate [Hz]	Purpose
MU20	0.8	$\mu 20i$	40	$t\bar{t}H$, $H \rightarrow WW, ZZ$, top, W’, Z’, $Z \rightarrow ll$
2MU6	0.2	$2\mu 10$, $2\mu 6 + \text{mass}$	10, 10	$H \rightarrow WW, ZZ$, B, $Z \rightarrow ll$
EM25i	12	e25i, $\gamma 60i$	40, 25	$t\bar{t}H$, $H \rightarrow WW, \gamma\gamma$ top, W’, Z’, $Z \rightarrow ll$, $W \rightarrow \nu l$
2EM15i	4	2e15i, $2\gamma 20i$	<1, 2	$H \rightarrow WW, ZZ, \gamma\gamma$ $Z \rightarrow ll$
J200	0.2	j400	10	QCD, new physics
3J90	0.2	3j165	10	QCD, new physics
4J65	0.2	4j110	10	QCD, new physics
J60+xE60	0.4	j70+xE70	20	Supersymmetry
MU10+EM15i	0.1	$\mu 10 + e 15i$	1	$H \rightarrow WW, ZZ$ $t\bar{t}$ fully leptonic

7. Conclusion and Outlook

The ATLAS experiment will run in the harsh environment of the LHC, with a high bunch-crossing frequency, large event size and high luminosity. In order to select interesting physics processes from the bulk of background and known physics processes, a multi-level trigger system has been designed, consisting of a hardware LVL1 trigger and the software levels LVL2 and EF (the HLT).

Almost all parts of the LVL1 trigger system are designed or even already built. For the HLT, the recently published Technical Design Report¹² marks an important step towards the final design. In addition, it has initiated a new round of trigger-performance studies. In parallel to the hardware and software activities connected to the development of the LVL1 trigger and the HLT, detailed studies of possible trigger menus for data taking in the LHC start-up phase are currently being performed in close collaboration with the ATLAS physics working groups.

All in all, the ATLAS trigger is on a promising path, clearly aiming for meeting all requirements necessary for smooth ATLAS data taking from 2007 onwards.

Acknowledgments

I would like to thank N. Ellis, S. Tapprogge, E. Eisenhandler and L. Nisati for their careful reading of the manuscript and all my ATLAS colleagues for their effort and support.

References

1. <http://www.cern.ch>
2. <http://atlas.web.cern.ch>
3. ATLAS Collaboration, *ATLAS First-Level Trigger Technical Design Report*, CERN/LHCC/98-014 (1998).
4. ATLAS Collaboration, *Calorimeter Performance Technical Design Report*, CERN/LHCC/96-40 (1996); *Liquid Argon Calorimeter Technical Design Report*, CERN/LHCC/96-41 (1996); *Tile Calorimeter Technical Design Report*, CERN/LHCC/96-42 (1996).
5. P. Hanke *et al.*, *The ATLAS Level-1 Calorimeter Trigger Preprocessor*, in Proceedings of the 5th Workshop on Electronics for the LHC Experiments, Snowmass, USA, (1999) 478.
6. A. Watson, *Updates to the Level-1 e/gamma and tau/hadron Algorithms*, ATL-DAQ-2000-046 (2000).
7. ATLAS Collaboration, *Muon Spectrometer Technical Design Report*, CERN/LHCC/97-22 (1997).
8. A. DiMattia and L. Luminari, *Performances of the Level-1 Trigger System in the ATLAS Muon Spectrometer Barrel*, ATL-DAQ-2002-008; A. DiMattia, *RPC Trigger Robustness: Status Report*, ATL-DAQ-2002-015.
9. A. Corre *et al.*, *A Demonstrator for the ATLAS Level-1 Muon To Central Trigger Processor Interface (MuCTPI)*, in Proceedings of the 6th Workshop on Electronics for the LHC Experiments, Cracow, Poland, (2000) 343.
10. I. Brawn *et al.*, *A Demonstrator for the ATLAS Level-1 Central Trigger Processor*, in

- Proceedings of the 3rd Workshop on Electronics for the LHC Experiments, London, England, (1997) 413.
11. R.E. Blair *et al.*, *A Prototype RoI Builder for the Second Level Trigger of ATLAS Implemented in FPGA's*, in Proceedings of the 5th Workshop on Electronics for the LHC Experiments, Snowmass, USA, (1999) 323.
 12. ATLAS Collaboration, *ATLAS High-Level Trigger, Data Acquisition and Controls Technical Design Report*, CERN/LHCC/03-022 (2003).
 13. M. Grothe *et al.*, *Architecture of the ATLAS High Level Trigger Event Selection Software*, arXiv:hep-ex/0306097, to be published in Proceedings of the 2003 Conference on Computing in High Energy and Nuclear Physics (CHEP2003), La Jolla, USA (2003).
 14. G. Comune *et al.*, *The Algorithm Steering and Trigger Decision mechanism of the ATLAS High Level Trigger*, arXiv:hep-ex/0306009, to be published in Proceedings of the 2003 Conference on Computing in High Energy and Nuclear Physics (CHEP2003), La Jolla, USA (2003).
 15. M. Elsing *et al.*, *Analysis and Conceptual Design of the HLT Selection Software*, ATL-DAQ-2002-013 (2002).
 16. S. Armstrong *et al.*, *An Overview of Algorithms for the ATLAS High Level Trigger*, to be published in Proceedings of the IEEE Real Time 2003 Conference and IEEE Transactions on Nuclear Science, Montreal, Canada (2003).
 17. <http://atlas.web.cern.ch/Atlas/GROUPS/SOFTWARE/OO/architecture/General>
 18. G. Barrand *et al.*, *Gaudi – A Software Architecture and Framework for Building HEP Data Processing Applications*, Comput. Phys. Commun.140 (2001) 45.
 19. ATLAS Collaboration, *ATLAS High-Level Trigger, DAQ and DCS Technical Proposal*, CERN/LHCC/2000-17 (2000).
 20. E. Moyse and A. Watson, *Performance and Validation of TrigT1Calo, the Offline Level-1 Calorimeter Trigger Simulation*, ATLAS Internal Note ATL-COM-DAQ-2003-010 (2003), to become ATLAS Note.
 21. M. Wielers, *Photon Identification with the ATLAS Detector*, ATL-PHYS-99-016 (1999);
 J. Baines *et al.*, *Identification of high p_T electrons by the Second Level Trigger of ATLAS*, ATL-DAQ-2000-003 (2000);
 R. Mommsen *et al.*, *Performance Studies for Electron and Photon Selection at the Event Filter*, ATL-DAQ-2000-007 (2000);
 P. Pralavorio, *Electron/Jet Separation with the ATLAS detector*, ATL-PHYS-99-015 (1999).
 22. J. Baines *et al.*, *Performance Studies of the High Level Electron Trigger*, ATLAS Internal Note ATL-COM-DAQ-2003-0020 (2003), to become ATLAS Note.
 23. A. DiMattia, *A muon trigger algorithm for Level-2 feature extraction*, ATL-DAQ-2000-036 (2000).
 24. S. Wheeler *et al.*, *Supervision of the ATLAS High Level Trigger System*, arXiv:hep-ex/0305093, to be published in Proceedings of the 2003 Conference on Computing in High Energy and Nuclear Physics (CHEP2003), La Jolla, USA (2003);
 S. Kolos *et al.*, *Online Monitoring software framework in the ATLAS experiment*, arXiv:hep-ex/0305096, to be published in Proceedings of the 2003 Conference on Computing in High Energy and Nuclear Physics (CHEP2003), La Jolla, USA (2003);
 M. Elsing and T. Schörner-Sadenius, *Configuration of the ATLAS Trigger System*, arXiv:hep-ex/0306046, to be published in Proceedings of the 2003 Conference on Computing in High Energy and Nuclear Physics (CHEP2003), La Jolla, USA (2003);
 G. Lehmann *et al.*, *The DataFlow System of the ATLAS Trigger and DAQ*, arXiv:cs.SE/0306101, to be published in Proceedings of the 2003 Conference on Com-

- puting in High Energy and Nuclear Physics (CHEP2003), La Jolla, USA (2003).
25. ATLAS Collaboration, *ATLAS Detector and Physics Technical Design Report*, CERN/LHCC/99-14 (1999).
 26. T. Schörner-Sadenius and S. Tapprogge, *ATLAS Trigger Menus for the LHC Start-Up Phase*, ATLAS Note ATL-DAQ-2003-004 (2003).